The effect of fluid–structural coupling on sound waves in an enclosure—Theoretical part

Jie Pan and David Alan Bies
Department of Mechanical Engineering, University of Adelaide, South Australia, 5001 Australia

(Received 15 February 1989; accepted for publication 21 September 1989)

This paper presents a theoretical investigation into the effect of the interaction between a sound field and its boundaries upon the characteristics of the sound field in an enclosure. Recent experimental measurements have shown that the boundaries of the sound field in a reverberation room cannot be correctly described in terms of a locally reactive normal acoustical impedance. Fluid–structural coupling must be taken into account if the mechanism of sound decay in the reverberation room is to be understood. A solution based on modal coupling analysis is obtained for the decay of sound waves in a panel–cavity system. The vibration of the system is resolved into a number of acoustical modes (including fluid and structural vibrations). The reverberation times and the resonance frequencies of different modes are calculated as a function of the modal parameters of the uncoupled panel and cavity. The effect of the panel characteristics on the decay behavior of the cavity sound field is investigated. The interesting phenomena of maximum sound absorption and resonance frequency "jump" are identified and interpreted in terms of the coupling behavior of the panel and cavity modes.

PACS numbers: 43.55.Br, 43.20.Ks, 43.55.Cs

INTRODUCTION

A. Statement of the problem

Fifty years ago, Morse[1] developed a theory of sound absorption for a rectangular room in terms of the locally reactive normal acoustics impedance. This theory is not only useful for predicting sound behavior in enclosures where the geometrical acoustic method does not apply, but it also suggests an entirely new way of looking at this problem. The significance of this pioneering work can be judged from the rapid progress that followed it in the field of room acoustics.

The assumption of locally reactive boundaries decreased the complexity of Morse's analysis and enabled the understanding of some basic physical properties of the acoustical modes in the room. Although most of the sound absorption material tested at the time behaved in a locally reactive manner, Morse hypothesized that future experiments might expose inadequacies in the locally reactive boundary assumption.

Experiments on the interaction between a sound field and its boundaries have demonstrated that the walls of a reverberation room are modally reactive, rather than locally reactive. Experimental evidence has also demonstrated that the modal coupling of the sound field and walls affects the decay times in the room.[2] In this case, the sound absorption is associated with a more complicated mechanism (modal coupling) and Morse's solution cannot provide an explanation for these experimental results, because the simplified locally reactive boundary assumption is not satisfied.

However, the significance of the fluid–structural coupling on sound absorption in a room and the relationship between the coupling properties and the sound field decay remain unknown until the mechanism of sound absorption by modally reactive boundaries is understood. The original question was associated with an architectural acoustics problem, but very soon the authors recognized that the research reported here stands on the new ground of fluid–structural coupling. Knowledge of modal coupling is certainly fundamental for solving the room acoustics problem and such knowledge may provide its own insights for architectural acoustics purposes as well.

B. Literature review

A literature survey of the fluid–structural coupling problem shows that a large amount of work has been done in the study of fluid and structural responses due to mutual coupling, but very little has been published on the effect of this coupling upon the decay behavior of the coupled system. However, in the case of architectural acoustics, the transient response is of fundamental importance.

Previous investigations into fluid–structural coupling have been motivated by the need to understand the effects of the vibrating boundaries on the fluid response, and a need to understand the acoustical loading of boundary structures by a cavity. Examples of the former are sound transmission into an enclosure from a vibrating boundary structure and sound radiation from a structure into the surrounding medium. These previous investigations cover a wide range of research and applications, but the underlying mechanism of the fluid–structural coupling remains the same. In the last 20 years, workers in a variety of fields have achieved a great deal of understanding of this mechanism.

The study of the effect of an underlying cavity on a plate originated from an interest in panel stability and panel excitation by aerodynamic noise. The model response of a cavity-backed plate was first investigated by Dowell and Voss.[3] Further investigations by Pretlove[4–6] and Guy[7] have pro-

 0001-4966/90/020691-17$00.80

gressively improved theoretical methods and physical insight. At about the same time as Dowell, Lyon[8] published his research on sound transmission into a rectangular enclosure through a panel. Since then, there has been a continuous effort (by Pretlove,[9] Khiolman,[10] Bhattacharya *et al.*,[11,12] Dowell *et al.*,[13] Guy *et al.*,[14,15] Naryannan and Shanbhag[16,17]) directed at improving the understanding of sound transmission through panels.

In addition to investigations of the simple rectangular panel–cavity system in Cartesian coordinates, the fluid–structural coupling problem has been studied in complex-shaped cavities and structures (particularly cylindrical shapes), which are closely related to the noise control problem in aircracft, piping systems, and water-borne structures. For example, the recent work of Fuller *et al.*[18,19] and Pope *et al.*[20,21] indicates the trends of aircraft noise control, and the work of Junger and Feit[22] presents a general treatment of the coupling problem (for cylindrical structures) in underwater acoustics.

Recently developed numerical techniques have made possible detailed investigation into the coupling in irregularly shaped cavities. After the energy formulation of the fluid–structural coupled system was developed by Gladwell and Zimmermann,[23] Craggs *et al.*[24,25] used a finite-element method to calculate the acoustical modes and resonance frequencies of a system. Since then this approach and other similar numerical methods (e.g., integral equation[26]) have been used to investigate control of noise inside a moving vehicle[27] and for sound transmission calculations. The paper by Nefske *et al.*[28] briefly reviewed the relevant research.

One particular aspect that is very often put aside is the effect of the fluid–structural coupling on the decay behavior of the coupled system. In the analysis of the coupling problem, the modal damping in the uncoupled subsystems is difficult to determine theoretically and is generally considered as an experimental parameter. Therefore, like other conventional approaches, the damping effect was normally neglected at first and, if necessary, the undamped system was modified later.

In the field of room acoustics, the decay behavior of an enclosure has been taken as an important measure of its acoustical quality, but the dependence of the decay on the fluid–structural coupling is still unknown. Under this circumstance, it is clear that an investigation into sound decay due to the coupling effect is necessary. The only paper to be found that attempted such analysis was published by Rogers[29] in 1939. In his paper, Rogers studied the absorption of sound due to the coupling between a one-dimensional sound field and pistonlike panels backed by a cavity. By comparing his result with the Sabine formula, he linked the sound absorption coefficient of the piston to the mechanical properties of the pistons and the cavity. He then discussed the extension of his results to the three-dimensional diffuse sound field. However, the response of boundary structures to a sound field is more complicated than that of a piston since the three-dimensional modal distribution of the sound field and the modal response of the boundary structure must also be taken into account.

Today, by using previous studies of the fluid–structural coupling problem as a basis, we are able to use "the modal coupling method" to analyze the sound absorption of modally reactive boundaries.

This article contains a theoretical investigation into the free-vibration behavior of a panel–cavity system. The behavior of the system is described in terms of acoustical modes. A solution for the decay time and resonance frequency of each acoustical mode is obtained by a modal coupling analysis. In this analysis, the characteristics of each mode is obtained by a modal coupling analysis. In this analysis, the characteristics of each mode can be determined in terms of the modal parameters of the uncoupled panel and cavity. By varying the properties of the test panel, the resonance frequency and the decay time of each acoustical mode can be changed. Relative maximum panel absorptions of the cavity-controlled modes are identified when the participating panel and cavity modes are well coupled. The effect of the panel damping and radiation loss to the outside space upon the decay time of the cavity-controlled modes is also discussed.

I. THEORETICAL MODEL

A. Description of the model

A panel–cavity coupled system is chosen as the theoretical model. This system consists of a rectangular box with slightly absorptive walls and a simply supported panel on top. The coordinates of the system are shown in Fig. 1.

B. General mathematical description

The properties of the coupled system can be obtained from its free-vibration solution, because the solution will give rise to modal properties, which are fundamental to the system. Once these modal properties are obtained, any response of the system to external excitation can be described in terms of these modal properties and the nature of the excitation.

In the discussion of the mode coupling problem in the following sections, the terminology "fluid–structural coupling" is used to describe the modal interaction between a sound field and the structure of its boundary. The sound field and the structural (i.e., test panel) vibration resulting

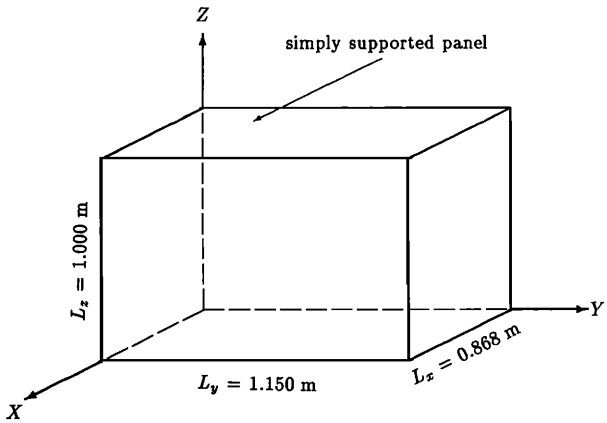

FIG. 1. Coordinate system of the panel-cavity model.

from this coupling are described in terms of acoustical modes. An acoustical mode is a mode of the entire panel–cavity system. An acoustical mode can be interpreted as the result of combining the uncoupled cavity modes (called "cavity modes") and the uncoupled panel modes (called "panel modes").

If we measure the relative amounts of energy contained in the two parts of the acoustical mode (i.e., in the cavity sound field and in the panel vibration), we can identify two types of acoustical modes as either "cavity controlled" or "panel controlled." A cavity-controlled mode has most of its energy stored in the cavity sound field, while a panel-controlled mode has most of its energy stored as panel vibrational energy.

In general, the free vibration problem of the system is described either in differential form with explicit specification of the interaction over the contacting boundaries of the fluid and the structure, or in integral form, which automatically includes the boundary conditions. The energy description (Hamiltonian) of the system will result in an integral equation and other integral forms can be derived directly from the differential form by the Green's function method. The physical meaning of the differential equations is straightforward, while the integral equations provide a convenient form for various numerical approximations.

C. Differential expressions

The free vibration of the panel–cavity system of Fig. 1 can be classified in three parts as follows.

(1) The sound field in the cavity is governed by a wave equation and its boundary conditions. In terms of an acoustic velocity potential Ψ, the wave equation for the free-vibration problem is

$$\nabla^2\Psi - \frac{1}{C_0^2}\frac{\partial^2\Psi}{\partial t^2} = 0, \tag{1}$$

where C_0 is the speed of sound in air. The air particle velocity $\mathbf{V}$ and sound pressure P are related to the velocity potential by $\mathbf{V} = \nabla\Psi$ and $P = -\rho_0(\partial\Psi/\partial t)$, respectively. The five walls of the cavity are assumed to be locally reactive and the boundary condition over the walls is described by the relation between the velocity potential and the specific acoustical impedance Z_A on the surfaces as follows:

$$\frac{\partial\Psi}{\partial n} = -\frac{\rho_0}{Z_A}\frac{\partial\Psi}{\partial t}. \tag{2}$$

In this equation, n indicates the normal direction on the surface of the boundary (positive outwards) and ρ_0 is the air density. If the boundaries are rigid, then $\partial\Psi/\partial n = 0$. The boundary condition over the flexible panel is determined by continuity of the normal air particle velocity and the normal panel velocity on the surface:

$$\frac{\partial\Psi}{\partial n} = \frac{\partial W}{\partial t}, \tag{3}$$

where W is the panel normal displacement.

(2) Different waveforms may exist in the panel, but only flexural waves have motions perpendicular to the surface that can cause radiation of sound into an adjacent medium. The behavior of the panel flexural motion is determined by the differential equation of motion, the boundary conditions along the panel edges, and the forces acting on the panel surfaces. The forces on the panel are due to the internal and external sound pressure. For a thin isotropic panel, the equation for flexural vibration is

$$\rho h\frac{\partial^2 W}{\partial t^2} + \frac{Eh^3}{12(1-\mu^2)}\nabla^4 W = \rho_0\left(\frac{\partial\Psi_E}{\partial t} - \frac{\partial\Psi}{\partial t}\right), \tag{4}$$

where ρ, E, μ, h, and Ψ_E are the density, Young's modulus, Poisson's ratio, thickness of the panel, and the acoustic velocity potential on the outside surface of the panel, respectively. The positive direction for panel displacement is outward. The panel edges are assumed to be simply supported for this analysis, but the general analysis used in this paper is not limited to simply supported panel edges.

(3) The velocity potential on the external surface of the panel is evaluated by the Rayleigh integral[30] for sound waves radiating from a baffled panel:

$$\Psi_E = -\frac{1}{2\pi}\int_{A_f}\frac{\partial W}{\partial t}\frac{\exp(-i\mathbf{k}\cdot\mathbf{r})}{r}\,ds_0, \tag{5}$$

where k is the wavenumber of the sound field and r is the distance from the source point (x_0,y_0) on the panel surface to the observation point (x,y). The time dependence term $\exp(i\omega t)$ has been suppressed in all expressions.

Many authors used transformation methods to solve the above equations.[4,10,12,15] Guy[15] finally presented a general analysis for the behavior of a cavity-backed panel. The transformation method (Fourier transformations to remove the spatial parameters and Laplace transformation to remove the time dependence) provides an exact solution to the nondissipative panel–cavity system. The properties of the system can be determined by searching the singularities (the poles) of the modal coefficients of the panel displacement. The response of the system to the external excitation can be obtained by additional investigation of the poles of the external force in the frequency domain. However, it is difficult to find the solution when damping of the system is present because the background modal damping is difficult to introduce in those cavity modes with nonzero modal index on the Z axis (see Fig. 1). These modes are implicitly represented in the solution.

D. Integral expressions

Equations (1) and (4) can be reduced to their corresponding integral equations by means of the Green's function method.[31] The integral equations for the acoustical velocity potential in an enclosure, and the panel displacement are equivalent to the original differential equations and automatically include the boundary conditions. This procedure requires a Green's function that satisfies the inhomogeneous equations (the original partial differential equations with a Dirac delta function as a point source). The Green's function can also be chosen to satisfy convenient boundary conditions to reduce the difficulties in the resulting boundary integral. The constructed Green's function is a transfer function from a point source to the velocity potential at an obser-

vation point in the cavity. By Gauss' theorem, the vibrating boundaries are mathematically taken as sources and the total contribution of these sources to the velocity potential is described by the summation (integration for the continuous source distribution) of the sources through their transfer functions over the whole of the boundaries. A sound field Green's function in the cavity, which satisfies the Neumann boundary condition, can be obtained by normal mode expansion:

$$G_A(\mathbf{r},\mathbf{r}_0;\omega) = \sum_N \frac{C_0^2}{\Lambda_N} \frac{\Phi_N(\mathbf{r})\Phi_N(\mathbf{r}_0)}{(\omega^2 - \omega_{aN}^2)}, \tag{6}$$

$$\Lambda_N = \int_V \Phi_N(\mathbf{r})\Phi_N(\mathbf{r})dv. \tag{7}$$

For the rectangular cavity, each normal mode can be written as

$$\Phi_N(\mathbf{r}) = \cos\left(\frac{l\pi x}{L_x}\right)\cos\left(\frac{m\pi y}{L_y}\right)\cos\left(\frac{n\pi z}{L_z}\right), \tag{8}$$

where (l,m,n) are the modal indices of the Nth cavity mode and ω_{aN} is the angular frequency of the Nth cavity mode; $\Phi_N(\mathbf{r})$ are the shape functions of the rigid wall modes. Here, they serve as base functions for the analysis of the sound field with flexible and absorptive walls.

The acoustical velocity potential in the cavity can be determined by integrating the distributed velocity contribution on the boundaries:

$$\Psi = -\int_A G_A \frac{\partial \Psi}{\partial n} ds_0 = -\int_{A_f} \frac{\partial W}{\partial t} G_A \, ds_0 + i\frac{\omega}{C_0}\int_{A_l} \beta \Psi G_A \, ds_0, \tag{9}$$

where $\beta = \rho_0 C_0 / Z_A$ is the specific acoustic admittance ratio on the wall surfaces A_l.

Similarly, the Green's function for a simply supported panel is

$$G_p(\mathbf{x},\mathbf{x}_0;\omega) = -\sum_M \frac{S_M(\mathbf{x})S_M(\mathbf{x}_0)}{\Lambda_M(\omega^2 - \omega_{pM}^2)}, \tag{10}$$

$$\Lambda_M = \int_{A_f} S_M(\mathbf{x})S_M(\mathbf{x})ds. \tag{11}$$

For a rectangular panel, each normal mode can be written as

$$S_M = \sin(u\pi x/L_x)\sin(v\pi y/L_y), \tag{12}$$

where ω_{pM} is the angular frequency of the Mth panel mode and (u,v) are the modal indices of the Mth panel mode; $\mathbf{x}$ and $\mathbf{x}_0$ are the observation and source points on the panel surface, respectively. Therefore the displacement of the panel due to the distributed sound pressures on the panel surfaces can be represented by

$$W = -i\frac{\rho_0 \omega}{\rho h}\int_{A_f} G_p(\mathbf{x},\mathbf{x}_0;\omega)(\Psi - \Psi_E)ds_0. \tag{13}$$

II. SOLUTION OF THE INTEGRAL EQUATIONS

The general mathematical methods for solving integral equations have been discussed by Morse and Feshbach.[32] To solve Eqs. (9) and (13) in the following sections, the methods of orthogonal expansion and of successive substitutions will be used. Dowell *et al.*[13] used the orthogonal expansion method to study the sound transmission problem between two rooms through a panel partition and the response of a panel–cavity system. The agreement of their measured and predicted panel resonance frequencies for various cavity depths demonstrates the success of the method for the coupling problem.

A. Method of orthogonal expansion

In this method, the acoustical velocity potential in the cavity $\Psi(\mathbf{r})$ is expanded in orthogonal functions Φ_N (rigid wall mode expression) and the panel displacement W is expanded in orthogonal panel mode functions S_M. The orthogonal cavity and panel modes are identical to those in the Green's functions for the cavity and the panel:

$$\Psi = \sum_N C_N \Phi_N, \tag{14}$$

$$W = \sum_M D_M S_M. \tag{15}$$

Substituting Eqs. (14) and (15) into Eqs. (9) and (13) and neglecting the panel radiation term, a series algebraic equations for each cavity mode N and for each panel model M are obtained as follows[13]:

$$(\lambda^2 - 2\zeta_{aN}\lambda + k_{aN}^2)M_N^a C_N + \lambda C_0 \sum_I B_{I,N} D_I = 0, \tag{16}$$

$$(\lambda^2 - 2\zeta_{pM}\lambda + k_{pM}^2)M_M^p D_M - \lambda C_0 \sum_J B_{J,M} C_J = 0, \tag{17}$$

where $M_N^a = \Lambda_N$ and $M_M^p = (phC_0^2/\rho_0)\Lambda_M$. $k_{aN} = \omega_{aN}/C_0$ is the wavenumber of the Nth cavity mode, $k_{pM} = \omega_{pM}/C_0$ is the "wavenumber" of the Nth panel mode and $\lambda = -ik$. In the panel wavenumber expression, the speed of sound in the denominator of the expression is for air rather than for the panel.

The damping of the Nth cavity modes is described by the specific acoustic admittance ratio β in Eq. (9). The boundary integral associated with β (i.e., $\Lambda_N^{-1}\int_{A_l}\beta\Phi_N\Phi_N \, ds$) becomes the modification term for the wavenumber of the Nth mode.[33] The integral can be split into two parts associated with the real and imaginary parts of β. As a result, the integral with conductance (real part of β) is associated with the damping constant ζ_{aN} of the Nth cavity mode. In general, ζ_{aN} depends upon cavity modal number. The effects of the specific acoustic admittance ratio β on ζ_{aN} and on the coupling of the cavity modes have been studied by many authors.[33,34] To simplify the effect of the locally reactive walls, ζ_{aN} are assumed to be independent of cavity mode number, and cavity modal coupling due to the distributed β has been neglected.

Each damping constant is used to represent the background absorption of each cavity mode and the Nth modal damping factor ζ_{aN} is related to the 60-dB decay time T_{aN} of the Nth cavity mode by $\zeta_{aN} = 6.91/C_0 T_{aN}$. The integral with susceptance (imaginary part of β) is related to the resonance frequency correction of the Nth cavity mode.

The mechanical damping of the test panel is usually represented by the complex Young's modulus and complex Poisson's ratio.[35] This produces complex angular resonance frequencies for the uncoupled panel.

The damping factor of the Mth panel mode, which is represented by ζ_{pM} in a manner similar to the cavity modal damping constant, can also be determined from the modal decay time of the Mth panel mode using $\zeta_{pM} = 6.91/C_0 T_{pM}$.

Here, $B_{M,N}$ is the modal coupling coefficient between the Mth panel mode and the Nth cavity mode:

$$B_{M,N} = \int_{A_f} S_M \Phi_N \, ds. \tag{18}$$

For the system of Fig. 1, the coupling coefficient between the Mth panel mode (u,v) and the Nth cavity mode (l,m,n) is

$$B_{M,N} = \begin{cases} (-1)^n \dfrac{A_f}{\pi^2} \dfrac{uv[(-1)^{l+u}-1][(-1)^{m+v}-1]}{(l^2-u^2)(m^2-v^2)}, \\ 0, \quad l = u \text{ and, or } m = v. \end{cases} \tag{19}$$

The modal coupling coefficient is a measure of the spatial match between panel and cavity modes. As noted by Pretlove[4] and Bhattacharya,[12] the coupling of the cavity modes and the panel modes is very selective. Table I shows the possible coupling modal pairs. Khilman[10] also estimated the coupling coefficient of a panel mode with all the possible cavity modes. He found that the coupling coefficient is large only for a very few cavity modes.

TABLE I. Selection rule for panel–cavity modal interaction (0, odd number; e, even number; n, arbitrary cavity modes index in Z direction) ($\surd$: $B_{M,N} \neq 0$).

Panel modes	Cavity modes (o,o,n)	(e,e,n)	(o,e,n)	(e,o,n)
(o,o)		$\surd$		
(e,e)	$\surd$			
(o,e)				$\surd$
(e,o)			$\surd$	

From Eqs. (16) and (17), a matrix can be constructed for the solution of the eigenvalues λ:

$$(\lambda^2 \mathbf{M} + \lambda \mathbf{L} + \mathbf{S})\mathbf{X} = 0, \tag{20}$$

where M is the inertia matrix, L is the coupling matrix, and S is the stiffness matrix. If only $N1$ cavity modes and $N2$ panel modes are used, then

$$\mathbf{M} = \begin{pmatrix} M_1^a & & & & & & \\ & \ddots & & & 0 & & \\ & & M_{N1}^a & & & & \\ & & & M_1^p & & & \\ & 0 & & & \ddots & & \\ & & & & & M_{N2}^p \end{pmatrix}, \tag{21}$$

$$\mathbf{L} = \begin{pmatrix} -2M_1^a\zeta_{a1} & & 0 & & C_0B_{1,1} & \cdots & C_0B_{1,N2} \\ 0 & \ddots & & & \vdots & \ddots & \\ & & -2M_{N1}^a\zeta_{aN1} & & C_0B_{N1,1} & \cdots & C_0B_{N1,N2} \\ -C_0B_{1,1} & \cdots & -C_0B_{N1,1} & & -2M_1^p\zeta_{p1} & & 0 \\ \vdots & \ddots & & & 0 & \ddots & \\ -C_0B_{1,N2} & \cdots & -C_0B_{N1,N2} & & & & -2M_{N2}^p\zeta_{pN2} \end{pmatrix}, \tag{22}$$

$$\mathbf{S} = \begin{pmatrix} M_1^a k_{a1}^2 & & & & & & \\ & \ddots & & & 0 & & \\ & & M_{N1}^a k_{aN1}^2 & & & & \\ & & & M_1^p k_{p1}^2 & & & \\ & 0 & & & \ddots & & \\ & & & & & M_{N2}^p k_{pN2}^2 \end{pmatrix}, \tag{23}$$

and X is the eigenvector of the system with all the unknown coefficients $(C_1,...,C_{N1}; D_1,...,D_{N2})$ as its components.

By using $N1$ cavity modes and $N2$ panel modes, Eq. (20) becomes an $(N1+N2)$ dimensional matrix equation, which gives $(N1+N2)$ eigenvalues $(\lambda_1,\lambda_2,...,\lambda_{N1+N2})$. The imaginary part of the eigenvalue λ_i is related to the resonance frequency of the ith acoustic mode $[f_i = \mathrm{Im}(\lambda_i)C_0/2\pi]$ and the real part is related to the damping constant (or the modal decay time) of the mode $[T_{i60} = 6.91/\mathrm{Re}(\lambda_i)C_0]$.

This solution shows that the sound field in the cavity and the response of the panel may be described in terms of the uncoupled cavity modes and panel modes with interactions between them. The interaction accounts for the structural vibration that disturbs the interior acoustical response, and also the acoustic pressure loadings that act on the panel. The coupling of the two sets of uncoupled modes is mathematically represented by matrix L.

Since this expression only requires the modal representation of the cavity and panel, various numerical techniques can be employed to find these parameters first when the shapes of the cavity and the panel are complicated. Then, coupling is introduced to obtain a new set of acoustical modes, which are represented in terms of the uncoupled modes.

By means of a matrix transformation,[36] the nonstandard eigenequation, Eq. (20), can be changed into a standard real eigenequation, but at the expense of doubling the dimension of the matrix. By introducing $\mathbf{Y} = \lambda \mathbf{X}$, Eq. (20) becomes

$$\begin{bmatrix} 0 & I \\ -\mathbf{M}^{-1}\mathbf{S} & -\mathbf{M}^{-1}\mathbf{L} \end{bmatrix} \begin{bmatrix} \mathbf{X} \\ \mathbf{Y} \end{bmatrix} = \lambda \begin{bmatrix} \mathbf{X} \\ \mathbf{Y} \end{bmatrix}. \tag{24}$$

This standard eigenvalue problem is solved by an IMSL package[37] in the following calculation.

For each eigenvalue, an eigenvector can be obtained. The components of this eigenvector are used to describe the distribution of the corresponding acoustical mode. For example, eigenvalue λ_i corresponds to the eigenvector $(C_{i1},...,C_{iN1},D_{i1},...D_{iN2})$. The sound field part of the ith acoustical mode can be written as

$$\Psi_i = \sum_N C_{iN}\Phi_N, \tag{25}$$

and the panel vibration part can be written as

$$W_i = \sum_M D_{iM}S_M. \tag{26}$$

B. Method of successive substitutions

The eigenvalues and eigenfunctions of the cavity-controlled modes of the coupled system can also be evaluated individually. For example, the complex wavenumber (eigenvalue) of the Nth cavity-controlled mode ξ_N can be calculated by the following expression, which is derived from the wave equation and Gauss' divergence theorem[32,38]:

$$\xi_N^2 = k_{aN}^2 + i\frac{\int_{A_f}\beta\Psi\Phi_N\,ds}{\int_V \Psi\Phi_N dv}\xi_N - \frac{\rho_0 C_0^2}{\rho h}\frac{\int_{A_f}\int_{A_f}\Psi G_p \Phi_N\,ds_0\,ds}{\int_V \Psi\Phi_N dv}\xi_N^2 + \frac{\rho_0 C_0^2}{\rho h}\frac{\int_{A_f}\int_{A_f}\Psi_E G_p \Phi_N\,ds_0\,ds}{\int_V \Psi\Phi_N dv}\xi_N^2. \tag{27}$$

Equation (27) shows that the eigenvalue of each cavity-controlled mode is represented by four terms. The first term is related to the eigenvalue of the corresponding cavity mode for the rigid wall condition. The second term is the contribution of the locally reactive boundaries. Morse[1] has investigated the effect of this term upon the eigenvalues of a rigid wall cavity. The third term is the contribution of the interaction of the interior sound field with the panel vibration, and the last term is the contribution due to the panel radiation into the external space.

The eigenfunction for the sound field part of the Nth cavity-controlled mode is

$$\Psi_N = \Phi_N - \int_{A_f}\frac{\partial W}{\partial t}G'_A ds_0 + i\frac{\omega}{C_0}\int_{A_l}\beta\Psi G'_A ds_0, \tag{28}$$

where the prime on the cavity Green's function indicates that the term involving Φ_N in the sum is omitted.

By including the damping of the cavity and panel modes (and neglecting the panel modal radiation effect, i.e., $\Psi_E = 0$), the approximate solution for the Nth eigenvalue ξ_N becomes

$$\xi_N^2 = k_{aN}^2 + 2i\zeta_{aN}\xi_N + \frac{1}{M_N^a}U_{N,N}\xi_N^2 + \sum_{N'\neq N}\frac{U_{N',N}U_{N,N'}}{M_N^a M_{N'}^a[\xi_N^2 - (k_{aN'}^2 + 2i\zeta_{aN'}\xi_N)]}\times\xi_N^4 + \cdots, \tag{29}$$

where

$$U_{N,N} = \sum_M \frac{C_0^2 B_{M,N}^2}{M_M^p[\xi_N^2 - (k_{pM}^2 + 2i\zeta_{pM}\xi_N)]}, \tag{30}$$

$$U_{N',N} = \sum_M \frac{C_0^2 B_{M,N'}B_{M,N}}{M_M^p[\xi_N^2 - (k_{pM}^2 + 2i\zeta_{pM}\xi_N)]}. \tag{31}$$

The third term on the right side of Eq. (29) is the contribution of the coupling of the examined cavity mode with all the panel modes. The fourth term is the contribution of the coupling of the examined cavity mode with other cavity modes through their interactions with panel modes.

The ξ_N^2 can be solved by successive approximation as follows:

$$\xi_{N(1)}^2 = k_{aN}^2 + 2i\zeta_{aN}k_{aN}, \tag{32}$$

$$\xi_{N(2)}^2 = k_{aN}^2 + 2i\zeta_{aN}\xi_{N(1)} + \frac{1}{M_N^a}U_{N,N}\xi_{N(1)}^2, \tag{33}$$

$$\xi_{N(3)}^2 = k_{aN}^2 + 2i\zeta_{aN}\xi_{N(2)} + \frac{1}{M_N^2}U_{N,N}\xi_{N(2)}^3$$

$$+\sum_{N'\neq N}\frac{U_{N',N}U_{N,N'}}{M^a_N M^a_{N'}\left[\xi^2_{N(2)}-(k^2_{aN'}+2i\zeta_{aN'}\xi_{N(2)})\right]}\times\xi^4_{N(2)}. \tag{34}$$

When the panel radiation term is taken into account, an extra term Δ^{Pr}_N should be added to the right side of Eq. (29). The first-order approximation of this term is obtained by using the first-order approximate panel displacement and neglecting the panel cross modes interaction:

$$\Delta^{Pr}_N=-\frac{iA_fC^4_0}{4M^a_N}\left(\frac{\rho_0}{\rho h}\right)^2\times\sum_M\frac{B^2_{M,N}[\sigma_{\rm Im}(M,N)-i\sigma_{\rm Re}(M,N)]}{(M^p_M)^2[\xi^2_N-(k^2_{pM}+2i\zeta_{pM}\xi_N)]^2}\xi^3_N, \tag{35}$$

where $\sigma_{\rm Re}(M,N)$ is the radiation efficiency of the M th panel mode at the resonance frequency of the Nth cavity-controlled mode:

$$\sigma_{\rm Re}(M,N)=\frac{2\xi^2_N}{\pi A_f}\int_{A_f}S_M(\mathbf{x}_1)S_M(\mathbf{x}_2)\frac{\sin(\xi_N r)}{\xi_N r}\,ds_1\,ds_2. \tag{36}$$

The calculation of the modal radiation efficiency of a simply supported rectangular panel has been discussed by Wallace[39] and Leppington *et al.*,[40] and r is the distance between point $\mathbf{x}_1$ and point $\mathbf{x}_2$ on the panel. Also, $\sigma_{\rm Im}(M,N)$ is associated with the contribution of the "virtual mass" of the M th panel mode:

$$\sigma_{\rm Im}(M,N)=\frac{2\xi^2_N}{\pi A_f}\int_{A_f}S_M(\mathbf{x}_1)S_M(\mathbf{x}_2)\frac{\cos(\xi_N r)}{\xi_N r}\,ds_2\,ds_2. \tag{37}$$

Pretlove[5] studied the "virtual mass" of a simply supported panel in air and pointed out that the effect of the virtual mass attached to the panel is negligibly small in all practical cases. When the panel radiation term is considered, a substitution method similar to that of Eqs. (31)–(33) is used by including Δ^{Pr}_N.

III. PROPERTIES OF THE SOLUTIONS

A. Convergence

The acoustical velocity potential Ψ [Eq. (9)] obtained by Green's function integral on the internal boundaries has discontinuous slope at the panel surface, because the selected Green's function satisfies the second-order homogeneous condition on the boundaries on the panel surface (i.e., $\partial G_A/\partial n=0$). This prescribed boundary condition for the Green's function has the result that $\partial\Psi/\partial n=0$ on the panel surface, but the boundary condition of the velocity potential Ψ at the panel surface has been defined by Eq. (3) as nonzero. Although only Ψ rather than $\partial\Psi/\partial n$ is used in the analysis, when the velocity potential is expanded as orthogonal functions (which are the same as those for the Green's function), this discontinuity may affect the speed of the convergence of the solution.

The acoustical velocity potential in the cavity can be represented by any set of orthogonal functions that are complete in the region of the cavity. However, when the chosen functions do not satisfy the boundary conditions (for example, the cosine functions that we have chosen do not satisfy the inhomogeneous Neumann condition on the panel surface), the speed of the convergence of the expansion (of the slope of the functions) to the exact value will depend upon the number of terms in the expansion and the position chosen for the evaluation. Near the boundary, more terms may be needed to achieve the convergence, but, away from the boundary, only a few terms may be needed to give a reasonable value.

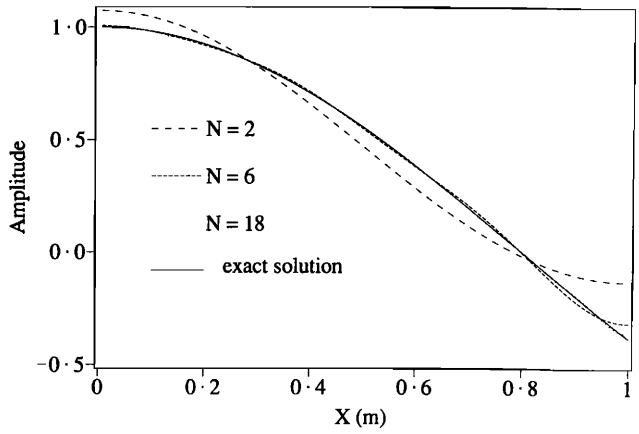

FIG. 2. The sound field distribution of the first mode in a tube terminated by a resonant piston. Exact sound field distribution and the approximated distribution by the first N terms of the base function $\cos(n\pi x/L_x)$, $(n=0,1,2,\ldots,N-1)$.

Taking the sound field in a one-dimensional tube (with length of $L_x=1$ m) as an example, the first mode for the two rigid ends can be simply represented by one function $\cos(\pi x/L_x)$ from the whole set of the cosine functions in the region $(0\leqslant x\leqslant L_x)$. If one end of the tube is terminated by a resonant piston, the shape of the first mode changes (see Fig. 2). {The exact solution for the resonance frequencies of the one-dimensional sound field terminated by a resonant piston (resonance frequency is f_0) can be obtained from $[1-(k_0/k)^2]=(v\rho_0/m_p)/[\cot(kL_x)/kL_x]$, where $k_0=2\pi f_0/C_0$, V is the volume of the tube, and m_p is the mass of the piston.

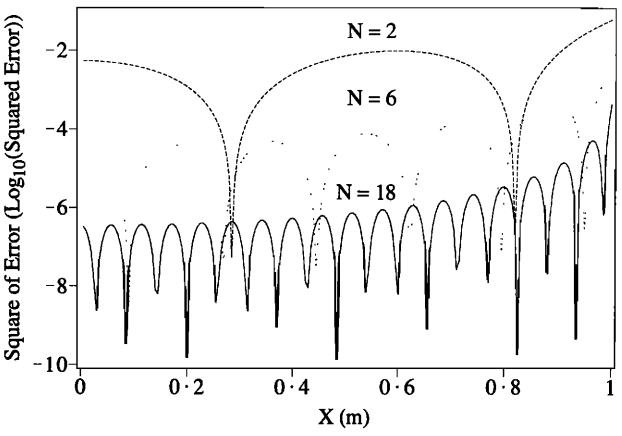

FIG. 3. Square of the amplitude error between the approximate sound field distribution and exact sound field distribution of the first mode.

In the calculation of Figs. 2 and 3, $f_0 = 340/\pi$ Hz, the radius of the tube is 0.05 m, $m_p = 0.05$ kg, and $L_x = 1$ m. The first resonance frequency of the tube with the piston is 106.3 Hz.} However, the mode shape can still be resolved into a set of cosine functions that are the normal modes for the rigid wall tube. Figure 3 shows the squared error of the approximated sound field distribution from the exact distribution in the tube. Increasing the number of the base functions improves the convergence of the calculation, but the convergency rate is different for different positions in the tube. Convergence is problem dependent, and numerical tests may be a proper way to evaluate it. Nefske *et al.*[28] estimated the convergence of the resonance frequencies of the sound modes in a piston-terminated tube as a function of the number of rigid wall modes. Dowell[13] pointed out that the sound pressure can still be determined correctly anywhere including the surface of the panel, even though the normal derivative of the expression for the normal modes expansion does not converge uniformly at the panel surface. Feshbach[31] also mentioned that the difficulty of the convergence will not exist for simple boundaries. All of this previous work suggests that the modal coupling approach can achieve good convergence.

B. Weak coupling

Weak coupling has been commonly assumed in the analysis of air-structural interaction problems.[41] It prescribes the state of the strength of the interaction of the subsystems in the coupled system. In general, if the energy involved in the interaction is much smaller than the energies in the subsystems, the coupling is described as weak. The motion of each subsystem in a weakly coupled system will not be essentially different from that of the uncoupled systems. The coupling only perturbs the state of the motion of the uncoupled systems. Mathematically, the coupled modes will be sufficiently represented by a limited number of the uncoupled cavity and panel modes.

When the panel and cavity are coupled, the mode shapes and the resonance frequencies of the panel and cavity are only slightly disturbed. Because of the low density of the air and the high stiffness of the panel, the radiation loading generally has little effect upon the panel vibration, and the actual motion of the panel normal to its surface is so small that the mode shapes of the sound field in the cavity will not be strongly affected. However, if the cavity in contact with the panel is very shallow and the panel is very light,[4] or the density of the surrounding medium is more dense than air, such as water,[42] the coupling may turn out to be strong, and big deformation of the resulting modes from the uncoupled panel and the cavity modes may be expected. In this situation, mode coupling analysis may be inadequate.

C. Well-coupled modes

When two subsystems are weakly coupled, it is usually expected that some modes in the uncoupled systems will play no important role in the coupling mechanism. In this case, the problem will be greatly simplified by neglecting these unimportant modes. In statistical energy analysis, the well-coupled modes concept has been used to select the modal pairs that dominate the coupling calculation of the two subsystems.[43,44] The condition for the well-coupled mode has been obtained[44] and is as follows:

$$2|\omega_{aN} - \omega_{pM}| < (\Delta\omega_{aN} + \Delta\omega_{pM}), \tag{38}$$

where $\Delta\omega_{aN}$ is the bandwidth of the Nth cavity mode, and $\Delta\omega_{pM}$ is the bandwidth of the Mth panel mode. In this analysis, the power transfer between those modal pairs that do not satisfy the condition given by Eq. (38) will be neglected, whatever their coupling coefficient might be. In the study of individual mode behavior, this criterion will also be useful for estimating the relative importance of the participating modal pairs. The modal coupling must also be taken into consideration, because there will be no energy transfer between two modes while their coupling factor is zero, even though their resonance frequencies are close. In this work, a transfer factor[45] that has been used in electrical coupling problems is used to decide the relative importance of different modes. The transfer factor of electrical coupling theory reinterpreted for the Nth cavity mode and Mth panel mode of the panel–cavity system may be written as

$$F_{M,N} = \{1 + [(\omega_{aN} - \omega_{pM})/2]^2 \, [1/B(M,N)^2]\}^{-1}, \tag{39}$$

where

$$B(M,N) = (\rho_0 C_0^2/\rho h \Lambda_N \Lambda_M)^{1/2} B_{M,N}. \tag{40}$$

When $|F_{M,N}| \cong 1$, the coupling is very important, but, if $|F_{M,N}| \ll 1$, the modes will be less affected by one another. In the analysis of two weakly coupled oscillators, the transfer factor is used to determine the maximum fraction of the energy transferred between the oscillators. Therefore, larger energy transfer is expected between the Nth cavity mode and the Mth panel mode when their transfer factor is large.

IV. COUPLING EFFECT ON THE ACOUSTICAL MODES

The solution of Eq. (24) or Eq. (27) depends upon the parameters of the uncoupled test panel and the cavity. The purpose of this section is to discuss how these parameters relate to the coupling and to the behavior of the coupled system, with emphasis on the resulting modal decay times.

A. Modal coupling coefficients

A coupling coefficient between a cavity and a panel mode is determined by the integral of their mode shapes on the contacting surface. The mode shapes of the panel, in turn, depend upon panel dimensions and the boundary conditions. Different boundary conditions will give rise to different mode shapes and to different coupling factors. In order to obtain a basic physical picture, we will confine the analysis to the simply supported edge condition for the panel, although similar analyses can be applied to more complicated boundary conditions.

B. Resonance distribution and panel modal density

It is well known that the energy transfer between two coupled oscillators depends upon the uncoupled resonance frequencies of each oscillator. The power flow from one oscillator to another increases as the difference of their reso-

nance frequencies decreases.[46] The panel–cavity system is interpreted as a multimode coupled system. The relative resonance frequencies of the coupled cavity and panel modes will also affect the energy transfer between them just as in the similar case of the two coupled oscillators. The modal density of the panel and the cavity at the examined frequencies will also affect the energy transfer, because the coupling is not only controlled by the two interacting panel and cavity modes, but is also affected by other modes of near resonance frequencies.

The resonance frequencies of the rigid wall cavity and of the simply supported panel are given by the following equations:

$$f_{l,m,n} = \frac{C_0}{2}\left[\left(\frac{l}{L_x}\right)^2 + \left(\frac{m}{L_y}\right)^2 + \left(\frac{n}{L_z}\right)^2\right]^{1/2}, \quad (41)$$

$$f_{u,v} = 0.458 C_L h \left[\left(\frac{u}{L_x}\right)^2 + \left(\frac{v}{L_y}\right)^2\right], \quad (42)$$

where C_L is the longitudinal speed of sound in the panel.

In the panel–cavity system, the resonance frequencies of the uncoupled modes can be adjusted by altering the dimensions of the cavity or the panel, or by changing the panel material (changing the longitudinal speed of sound in the panel). For the model shown in Fig. 1, the cavity dimensions are fixed but the test panel may be varied. In this analysis, the resonance frequencies of panel modes are altered by changing the panel thickness. The panel is assumed to be aluminum.

The thickness h of a panel with fixed surface area A_f and longitudinal wave speed C_L is related to the modal density of the panel by

$$n_P = \sqrt{3} A_f / C_L h. \quad (43)$$

Panel modal density is used to characterize the test panel. The modal density not only gives the average number of panel modes in a particular frequency band but also, together with the shape and boundary conditions of the panel, determines the resonance frequencies. The average number of the panel modes in the region of a resonance frequency of a cavity mode governs the overall nature of the coupling behavior, while the distribution of panel resonance frequencies determines the details of the coupling effect. The modal densities of the cavity and of two aluminum panels of different thicknesses are plotted in Fig. 4. The first few resonance frequencies of the cavity modes are within the frequency range from 150–280 Hz. When the panel modal density is very small, very few or no panel modes will couple with the cavity modes. As panel modal density becomes higher, more panel modes may participate in the coupling with cavity modes.

The properties of the first six cavity-controlled acoustical modes have been calculated as functions of panel modal density by the orthogonal expansion method [Eq. (24)]. Forty panel modes and 40 cavity modes have been used. All cavity modes are assumed to have a 15-s decay time, and all panel modes are assumed to have a 0.5-s decay time. The panel radiation is neglected. Figure 5 shows the variation in the decay time of some acoustical modes with panel modal density. When the panel modal density is high, and particularly for those panel modal densities where no panel modes are well coupled with the cavity mode, the accuracy of the results from this method is limited because of the limited number of modes used in the calculation. There are two extreme conditions of cavity–panel mode coupling. The first one is where a panel mode and a cavity mode are well cou-

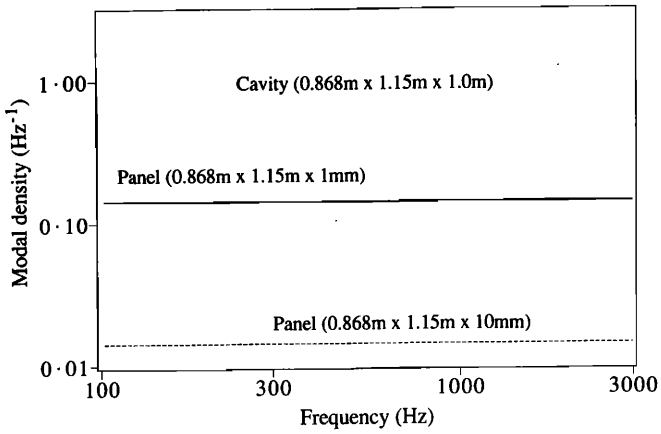

FIG. 4. Modal densities of the cavity and of two panels (aluminum panel $C_L = 5150$ m/s, 1 mm and 10 mm thick).

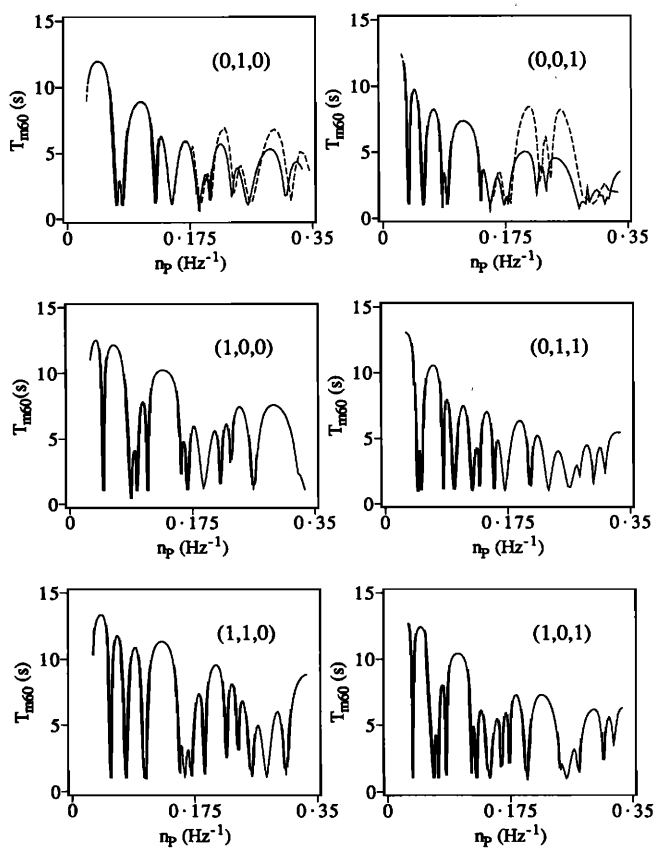

FIG. 5. Decay times of the first few cavity-controlled modes. - - -, orthogonal expansion method; —, successive iteration method ($T_{aN} = 15.0$ s and $T_{pM} = 0.5$ s). Each mode is identified according to the mode number of its dominant cavity mode component.

pled. In this case, the energy transfer between the sound field and the panel is almost entirely between these two modes. The behavior of the resultant acoustic mode and the energy flows between the different parts of the modes is well approximated by considering the coupling of a few modes and even when only including those two well-coupled modes. The second condition is where none of the panel modes is well coupled with the cavity mode. For this case, the energy transfer from the cavity mode is distributed over many panel modes, and the cavity-controlled acoustical mode contains components from many panel cavity modes of similar importance. Therefore, if only a small number of uncoupled modes is used in the analysis, some important modes may be excluded and errors may develop in the calculation of modal decay time. For these situations, the alternative method of successive iteration [Eq. (29)] has been used, because the number of panel modes is not limited by the computer memory capacity in this method. For example, 100 panel modes were used in the calculation of Fig. 5.

It is shown in Fig. 5 that, as the panel modal density is increased, the decay time of each mode has many relative minima. On the average, the decay time is longer in the low panel density region, and it becomes shorter as the panel modal density is increased. Figure 6 shows the transfer factor between cavity mode (0,0,1) and the first 14 panel modes (with nonzero coupling coefficients) as a function of panel modal density. In the region of the maximum values of the transfer factor, there is large energy transfer and maximum sound absorption by the panel. These peaks correspond to the decay time minima of the cavity-controlled mode (0,0,1) in Fig. 5.

When the panel modal density is small, only very few panel modes lie in the effective frequency region of the examined cavity mode and the energy transfer of the cavity mode into the panel will usually be dominated by a single panel mode. The influence of the higher-order panel modes upon the energy transfer is small. This is shown in Fig. 6. Unless one panel mode happens to satisfy the well-coupled condition with the examined cavity mode, the coupling between the cavity mode and the panel is generally very poor. Therefore, in this region of panel modal density, the modal decay time is long except for a few special regions where the well-coupled condition is satisfied. When the panel modal density becomes high, Fig. 6 shows that more panel modes (both low-order and high-order) participate in the coupling with the examined cavity mode. In this case, the cavity mode will have more panel modes to couple with. Therefore, on average, the resulting cavity-controlled modes have smaller decay times.

The details of the calculated modal decay curves (Fig. 5) in the region of minimum decay time are of special interest. The minimum modal decay time indicates maximum sound absorption by the panel. As panel modal density increase within this region, the resonance frequency of the cavity-controlled mode "jumps" to a higher frequency (see Fig. 7).

In order to explain the physical mechanism of this behavior, we must compare the motion of the panel with the motion of the sound field and the panel energy with the energy in the sound field. A calculation of the eigenvector of an acoustical mode from Eq. (20) can provide some insight into this relative motion and this relative energy content. The eigenvector of an acoustical mode determines the distribution of the sound field and the distribution of the panel vibration for that mode according to Eqs. (25) and (26).

The relative motion of the sound field and the panel vibration of the Nth acoustical mode are described by the specific acoustical transfer impedance Z_{apN}, which is sound

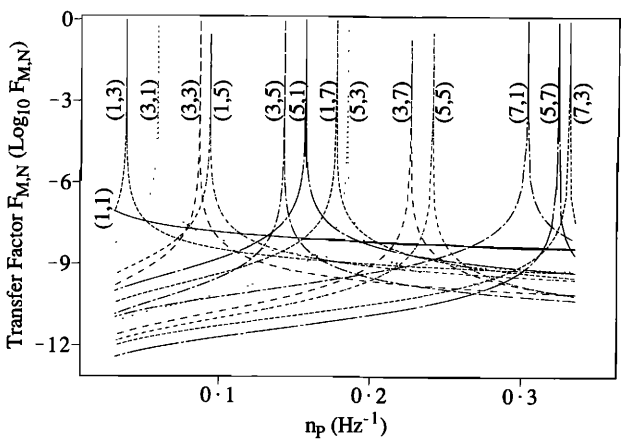

FIG. 6. The transfer factor $F_{M,N}$ between (0,0,1) cavity mode and panel modes as a function of panel modal density.

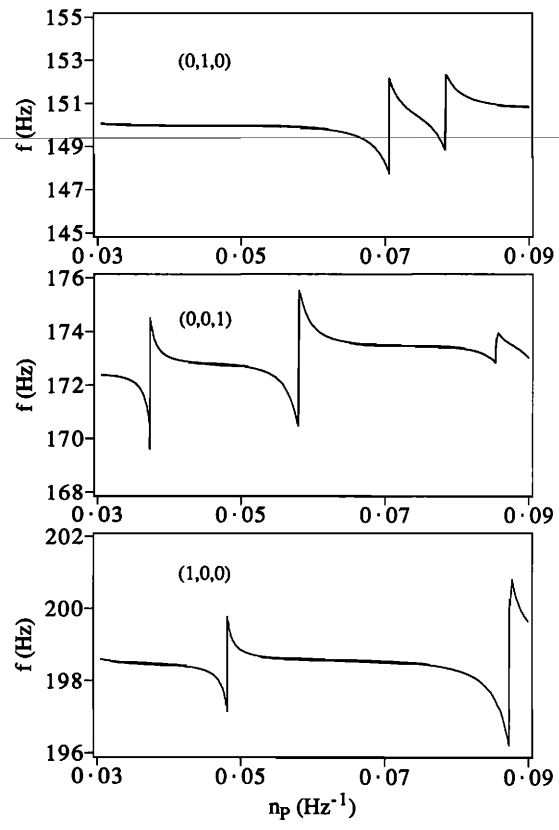

FIG. 7. Resonance frequencies of the first few cavity-controlled modes as a function of panel modal density, calculated by successive iteration method ($T_{aN} = 15.0$ s and $T_{pM} = 0.5$ s).

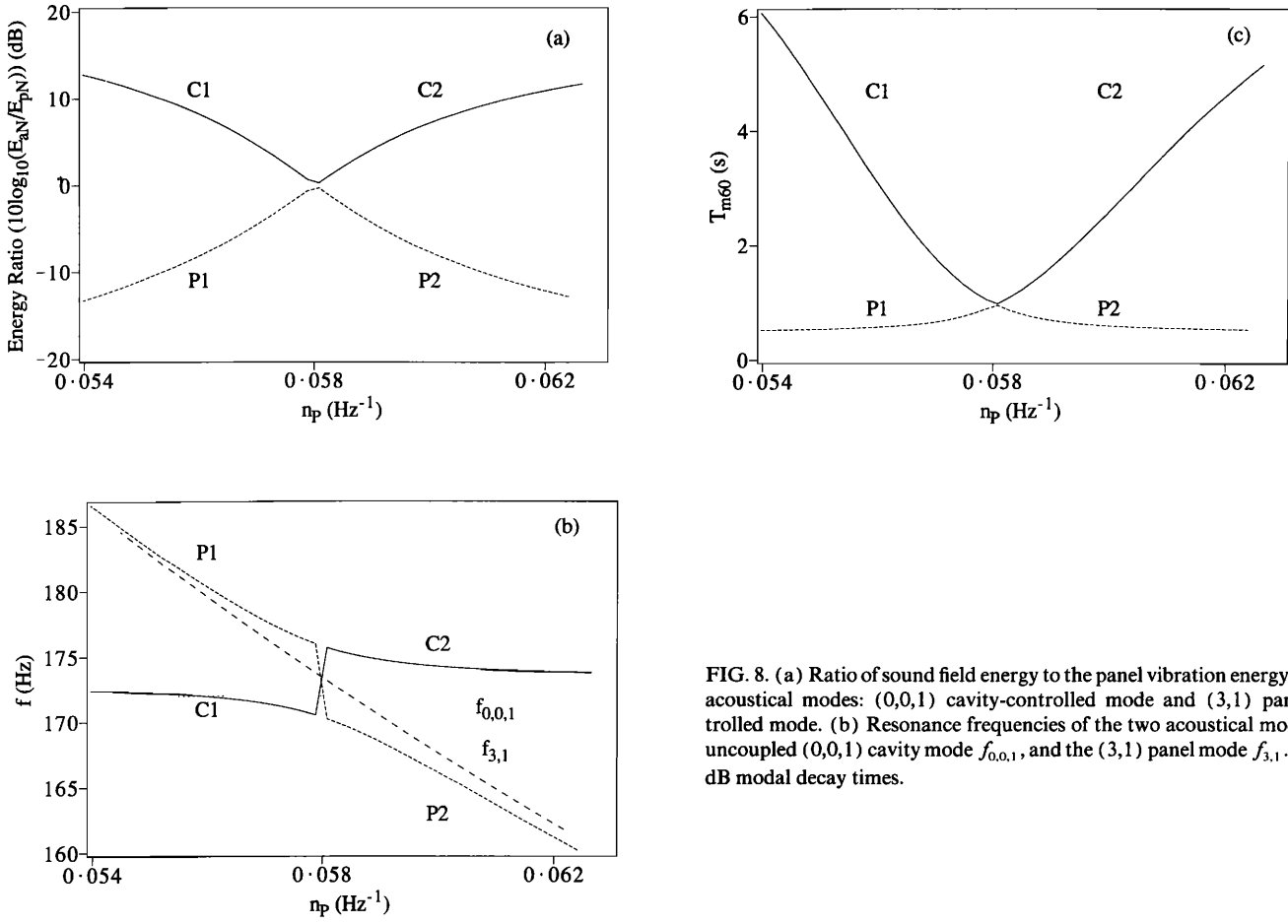

FIG. 8. (a) Ratio of sound field energy to the panel vibration energy for two acoustical modes: (0,0,1) cavity-controlled mode and (3,1) panel-controlled mode. (b) Resonance frequencies of the two acoustical modes, the uncoupled (0,0,1) cavity mode $f_{0,0,1}$, and the (3,1) panel mode $f_{3,1}$. (c) 60-dB modal decay times.

pressure divided by panel velocity. In terms of the acoustical velocity potential Ψ_N and the displacement W_N of the Nth mode, Z_{apN} is written as

$$Z_{apN} = -\rho_0(\Psi_N/W_N). \tag{44}$$

When Ψ_N is evaluated at the same point as W_N, Z_{apN} is the specific acoustical impedance at this point.

Similarly, the ratio of sound field energy to panel vibration energy E_{aN}/E_{pN} of the Nth mode is given by

$$\frac{E_{aN}}{E_{pN}} = \frac{1}{C_0^2}\frac{\rho_0 V}{\rho h A_f}\frac{\langle \overline{\Psi_N \Psi_N^*} \rangle}{\langle \overline{W_N W_N^*} \rangle}, \tag{45}$$

where Ψ_N^* and W_N^* are the complex conjugates of Ψ_N and W_N, respectively.

The energy ratios of two selected acoustical modes are shown in Fig. 8(a) as a function of panel modal density. The resonance frequencies and the 60-dB decay times of these two modes are shown in Figs. 8(b) and (c). For comparison, the resonance frequencies of the corresponding cavity mode and panel mode are also shown in Fig. 8(b). In each case, the solid curve in Fig. 8 represents the cavity-controlled mode and consists of two parts labeled C1 and C2. Likewise, the dashed curve represents the panel-controlled mode and is labeled P1 and P2. In each case, the two curves meet at a point where *sound* absorption of the cavity-controlled mode is maximum. When not in the vicinity of the point of maximum sound absorption [which corresponds to a peak in Fig. 6, e.g., (3,1) in this case], the difference between a cavity-controlled mode and a panel-controlled mode can easily be distinguished from the energy ratio, but, near this point, the energy ratios of the two types of modes are indistinguishable. Near the maximum sound absorption point, each part (panel and cavity) of the panel-controlled mode and of the cavity-controlled mode has the same amount of energy.

Therefore, for white noise excitation in the cavity, we expect to find two spectral peaks in the sound field when the modal density of the panel is close to the value for minimum sound absorption and the amplitudes of these peaks will be approximately equal.

The curves in Fig. 8(a)–(c) were obtained by considering 40 cavity modes and 40 panel modes. Table II lists the coefficient amplitudes of the uncoupled modes for a panel modal density of $n_P = 0.056$ Hz^{-1}. It shows that the cavity part of the vibrating system is dominated by the (0,0,1) cavity mode, and the panel part is dominated by the (3,1) panel mode. Therefore, it is convenient to call these acoustical modes the "(0,0,1) cavity-controlled mode" and the "(3,1) panel-controlled mode."

The curves in Fig. 8(a) also show that the "P2" part of the panel-controlled mode is a continuation of the "C1" part of the cavity-controlled mode. Similarly, the "C2" part of the cavity-controlled mode is a continuation of the "P1" part of the panel-controlled mode.

TABLE II. Amplitudes of the components of (0,0,1) cavity-controlled mode and the (3,1) panel-controlled mode ($h = 6$ mm). Panel modal density $n_P = 0.056\ \text{Hz}^{-1}$.

Cavity-controlled mode				Panel-controlled mode			
sound field		panel vibration		sound field		panel vibration	
(l,m,n)	amplitude	(u,v)	amplitude	(l,m,n)	amplitude	(u,v)	amplitude
(0,0,0)	0.378	(1,1)	2.71×10^{-02}	(0,0,0)	5.64	(1,1)	3.46×10^{-02}
(0,1,0)	5.75×10^{-14}	(1,2)	1.24×10^{-17}	(0,1,0)	6.05×10^{-13}	(1,2)	2.40×10^{-17}
(0,0,1)[a]	238.	(2,1)	6.33×10^{-17}	(0,0,1)[a]	120.	(2,1)	1.71×10^{-16}
(1,0,0)	4.31×10^{-13}	(1,3)	1.57×10^{-02}	(1,0,0)	1.69×10^{-12}	(1,3)	7.93×10^{-03}
(0,1,1)	3.65×10^{-14}	(2,2)	1.04×10^{-17}	(0,1,1)	6.35×10^{-13}	(2,2)	5.65×10^{-17}
(1,1,0)	9.95×10^{-16}	(2,3)	3.18×10^{-15}	(1,1,0)	1.05×10^{-14}	(2,3)	3.64×10^{-15}
(1,0,1)	9.63×10^{-14}	(3,1)[a]	9.74×10^{-02}	(1,0,1)	1.07×10^{-13}	(3,1)[a]	0.355
(0,2,0)	0.437	(1,4)	2.59×10^{-16}	(0,2,0)	1.92	(1,4)	9.64×10^{-15}
(1,1,1)	1.16×10^{-15}	(3,2)	9.14×10^{-16}	(1,1,1)	6.60×10^{-15}	(3,2)	3.10×10^{-14}
(0,0,2)	0.252	(2,4)	6.11×10^{-18}	(0,0,2)	4.28	(2,4)	2.95×10^{-17}
(0,2,1)	0.586	(3,3)	2.15×10^{-03}	(0,2,1)	2.53	(3,3)	1.19×10^{-03}
(1,2,0)	6.68×10^{-14}	(1,5)	2.96×10^{-03}	(1,2,0)	8.43×10^{-14}	(1,5)	1.83×10^{-03}
(0,1,2)	7.42×10^{-13}	(4,1)	9.44×10^{-18}	(0,1,2)	1.14×10^{-13}	(4,1)	2.87×10^{-17}
(2,0,0)	1.42	(3,4)	1.89×10^{-19}	(2,0,0)	4.58	(3,4)	4.68×10^{-18}
(1,0,2)	2.84×10^{-14}	(2,5)	5.16×10^{-18}	(1,0,2)	3.29×10^{-14}	(2,5)	1.06×10^{-17}
(1,2,1)	1.04×10^{-13}	(4,2)	8.36×10^{-19}	(1,2,1)	1.27×10^{-13}	(4,2)	2.38×10^{-18}
(2,1,0)	1.30×10^{-14}	(4,3)	5.79×10^{-19}	(2,1,0)	6.65×10^{-14}	(4,3)	6.57×10^{-18}
(1,1,2)	4.33×10^{-16}	(1,6)	1.08×10^{-18}	(1,1,2)	6.35×10^{-16}	(1,6)	6.69×10^{-18}
(2,0,1)	2.32	(3,5)	3.31×10^{-04}	(2,0,1)	7.41	(3,5)	1.58×10^{-04}
(0,3,0)	4.22×10^{-15}	(2,6)	1.56×10^{-17}	(0,3,0)	9.37×10^{-14}	(2,6)	1.24×10^{-17}
(0,2,2)	0.294	(4,4)	1.66×10^{-17}	(0,2,2)	1.25	(4,4)	2.84×10^{-17}
(2,1,1)	2.24×10^{-14}	(5,1)	8.03×10^{-04}	(2,1,1)	1.13×10^{-13}	(5,1)	3.37×10^{-04}
(0,3,1)	8.35×10^{-15}	(5,2)	2.29×10^{-17}	(0,3,1)	1.60×10^{-13}	(5,2)	2.23×10^{-17}
(1,3,0)	7.14×10^{-16}	(1,7)	4.17×10^{-04}	(1,3,0)	2.10×10^{-15}	(1,7)	2.45×10^{-04}
(2,2,0)	0.456	(3,6)	1.64×10^{-17}	(2,2,0)	1.83	(3,6)	1.54×10^{-17}
(1,2,2)	6.19×10^{-14}	(5,3)	1.80×10^{-04}	(1,2,2)	7.87×10^{-14}	(5,3)	9.77×10^{-05}
(0,0,3)	9.45×10^{-02}	(4,5)	9.24×10^{-18}	(0,0,3)	1.57	(4,5)	3.32×10^{-17}
(1,3,1)	8.17×10^{-16}	(2,7)	2.92×10^{-17}	(1,3,1)	9.68×10^{-16}	(2,7)	1.10×10^{-17}
(2,0,2)	1.48	(5,4)	1.88×10^{-17}	(2,0,2)	4.70	(5,4)	2.56×10^{-17}
(2,2,1)	0.802	(4,6)	7.27×10^{-17}	(2,2,1)	3.22	(4,6)	8.00×10^{-17}
(0,1,3)	3.50×10^{-15}	(6,1)	3.57×10^{-17}	(0,1,3)	4.68×10^{-14}	(6,1)	7.32×10^{-17}
(2,1,2)	1.56×10^{-14}	(3,7)	8.46×10^{-05}	(2,1,2)	7.93×10^{-14}	(3,7)	3.93×10^{-05}
(1,0,3)	1.31×10^{-14}	(1,8)	7.24×10^{-18}	(1,0,3)	1.59×10^{-14}	(1,8)	3.31×10^{-17}
(0,3,2)	5.03×10^{-15}	(6,2)	2.62×10^{-17}	(0,3,2)	1.10×10^{-13}	(6,2)	1.42×10^{-16}
(1,1,3)	3.75×10^{-16}	(5,5)	6.18×10^{-05}	(1,1,3)	7.51×10^{-16}	(5,5)	3.11×10^{-05}
(3,0,0)	4.23×10^{-15}	(2,8)	5.42×10^{-17}	(3,0,0)	2.77×10^{-15}	(2,8)	6.50×10^{-17}
(0,2,3)	0.160	(6,3)	3.83×10^{-17}	(0,2,3)	0.674	(6,3)	2.87×10^{-17}
(0,4,0)	6.37×10^{-02}	(4,7)	5.55×10^{-17}	(0,4,0)	0.117	(4,7)	1.36×10^{-16}
(2,3,0)	2.76×10^{-15}	(6,4)	3.63×10^{-18}	(2,3,0)	2.62×10^{-14}	(6,4)	6.39×10^{-17}
(1,3,2)	9.26×10^{-16}	(3,8)	2.00×10^{-17}	(1,3,2)	1.18×10^{-15}	(3,8)	3.30×10^{-17}

[a] Dominant modes.

The minimum decay time of the (0,0,1) cavity-controlled mode (see in Figs. 8 and 5) in the region ($0.054\ \text{Hz}^{-1} < n_P < 0.062\ \text{Hz}^{-1}$) is due mainly to the coupling of the (0,0,1) cavity mode and the (3,1) panel mode. In this region, the transfer factor of these modes has a maximum (Fig. 6). This coupling of the cavity mode and the panel mode strongly affects a *pair* of acoustical modes, one of which is the (0,0,1) cavity-controlled mode and the other is the (3,1) panel-controlled mode.

The resonance frequencies of the cavity-controlled mode and the panel-controlled mode in Fig. 8(b) show some interesting changes in the minimum decay time region. On the left of the minimum point, the resonance frequency of the (0,0,1) cavity-controlled mode is lower than that of (0,0,1) uncoupled cavity mode, but the resonance frequency of the (3,1) uncoupled panel-controlled mode is higher than that of the (3,1) panel mode. On the right side of this point, these inequalities are reversed. The resonance frequencies "jump" across the minimum decay time point. This "jump" can be partly explained by the phase change of the specific acoustical transfer impedance.

The coupling of a cavity and a panel mode is analogous to the coupling of two single degree of freedom oscillators. As is well known,[46] such coupling produces two new coupled modes in which the oscillators either move in phase at a resonance frequency lower, or in opposite phase at a resonance frequency higher than that of either oscillator taken individually. This indicates that the jump of the resonance frequency across the minimum decay time point associated with a jump in the phase of the specific acoustical transfer impedance.

Figure 9 (a1) and (a2) shows the calculated magnitude

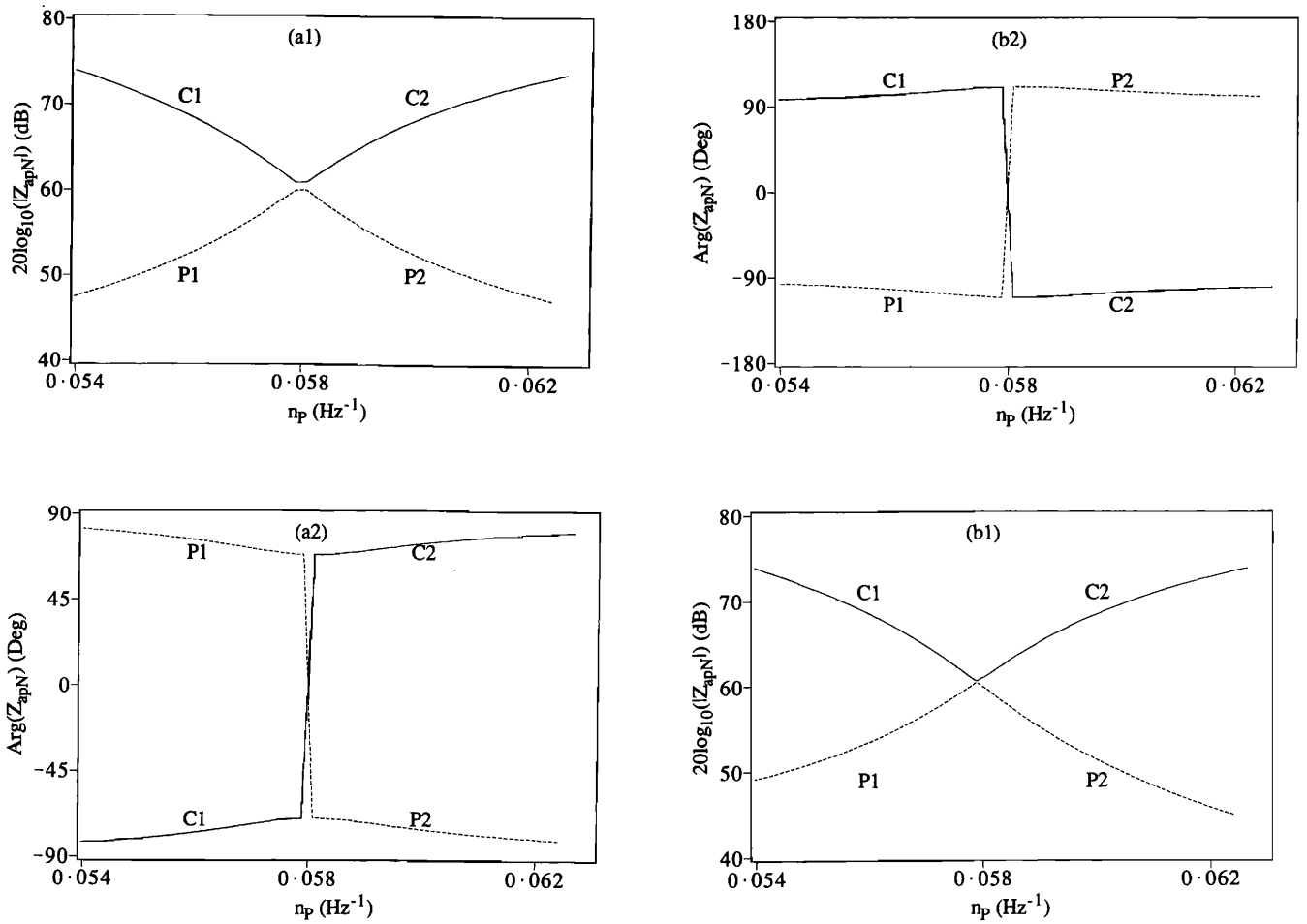

FIG. 9. (a1) and (a2): Acoustical specific transfer impedance of two acoustical modes [from (0.868, 1.150, 0.0)–(0.434, 0.575) m]. (b1) and (b2): Acoustical specific impedance at (0.434, 0.575). —, cavity-controlled mode (0,0,1); - - -, panel-controlled mode (3,1). [$|Z_{apN}|$ and $\arg(Z_{apN})$ are the amplitude and the phase angle of Z_{apN}].

and phase of the specific acoustical transfer impedance between location (0,0,0) m in the cavity and location (0.434, 0.575) m on the panel for the two acoustical modes as a function of the panel modal density. Figure 9 (b1) and (b2) shows the calculated magnitude and phase of the specific acoustical impedance of the panel surface at (0.434, 0.575) m for the same modes. Both the cavity-controlled mode and the panel-controlled mode have an impedance phase jump at the point of maximum sound absorption.

This phase jump indicates a change of the impedance state. (An impedance can be in a stiffness-, resonance-, or mass-controlled state.) However, unlike the coupling of two single degrees of freedom oscillators, the transfer impedance is a function of location and so the phase of the specific acoustical impedance varies over the panel surface. At one position, Z_{apN} could be mass controlled, and at another position it could be stiffness controlled. Therefore, whether the resulting resonance frequency of the cavity-controlled acoustical mode will be higher or lower than that of the uncoupled cavity mode depends upon the integrated contribution of the distributed specific acoustic impedance from every point on the panel surface. Referring to Figs. 8 and 9, it is clear that the "P2" part of the panel-controlled mode is a continuation of the "C1" part of the cavity-controlled mode, and that the "C2" part of the cavity-controlled mode is a continuation of the "P1" part of the panel-controlled mode. The continuation change from curve P1 to curve C2 and from curve C1 to curve P2 indicates that P1 and C2 represents just one acoustical mode and that "C1" and "P2" represent a second acoustical mode. As the panel modal density increases and passes through the maximum sound absorption point, the first acoustical mode changes from cavity controlled to panel controlled. The second acoustical mode is initially panel controlled, but, when it crosses the maximum sound absorption point, it becomes cavity controlled.

If we only measure the sound-pressure level in the cavity or if we only measure the panel acceleration, then we only observe one part of the coupled system. In a measurement of the cavity sound field, it is the cavity-controlled modes that are most easily observed. Naturally, when the panel vibration is measured, the panel-controlled modes are easier to resolve. Experimentally, there is a jump in phase of the transfer impedance and resonance frequency of the observed mode as the panel modal density is varied across the maxi-

mum sound absorption point. However, this jump is due to two simultaneous transitions. One transition is of a panel-controlled mode into a cavity-controlled mode, and the other is from a cavity-controlled mode into a panel-controlled mode.

C. Panel internal damping

The mechanical damping of the panel is represented in the calculation by the modal decay times of the uncoupled panel modes. The decay time of a cavity-controlled mode can be directly related to the modal decay time of the uncoupled panel. Figures 10 and 11 show, respectively, the resonance frequencies and modal decay times of the first few cavity-controlled modes as a function of the decay time of the panel modes (T_{pM}). In the calculation, the thickness of the aluminum panel is 6 mm and the decay time of the uncoupled modes is 15 s. The decay time of every uncoupled panel mode is assumed to be equal. The resonance frequencies of the cavity-controlled modes vary as the panel damping increases, but eventually they approach the uncoupled cavity resonance frequencies. As the panel damping increases (T_{pM} decreases), the decay times of the cavity-controlled modes decrease and approach a minimum. After this minimum, the decay times increase and tend to those of the uncoupled cavity modes.

Panel damping is a measure of not only the ability of the panel to dissipate energy, but also its tendency to resist acquiring vibrational energy. Until the minimum decay time is reached, more and more energy is dissipated in the panel as its damping is increased. As the damping is increased further, it effectively restricts the motion of the panel and eventually the panel becomes rigid. Therefore, no energy will be transferred from the sound field in the cavity into the panel, and the modal charactersitics of the cavity will not be affected.

The resonance frequencies and decay times of each acoustical mode (Figs. 10 and 11) have different characteristics. For example, the curves in Fig. 10 are monotonic with the exception of one, which has a maximum. According to Eq. (29), the first-order approximation of the panel influence on the eigenvalue of the Nth cavity-controlled mode is described by $U_{N,N}$ [Eq. (30)]. The real part of $U_{N,N}$ modifies the resonance frequency of the mode, and the imaginary part of $U_{N,N}$ affects its modal decay time; $U_{N,N}$ contains the contributions of all the panel modes. Among the nonzero terms in the summation of Eq. (30), those panel modes which have lower resonance frequencies than that of the cavity mode make a positive contribution (increase) to the resulting resonance frequency of the acoustical mode. On the other hand, the panel modes with higher frequencies make a negative contribution (decrease) to the resonance frequency. The shift in resonance frequency is due to the combined effect of all the panel modes. Figure 12 shows the first few nonzero terms in $U_{N,N}$ that were used for the calculation of the eigenvalue of the (0,0,1) cavity-controlled mode shown in Fig. 10. For very small panel damping ($T_{pM} \approx 10$ s), the real part of the modification term $U_{N,N}$ for the (1,1) and

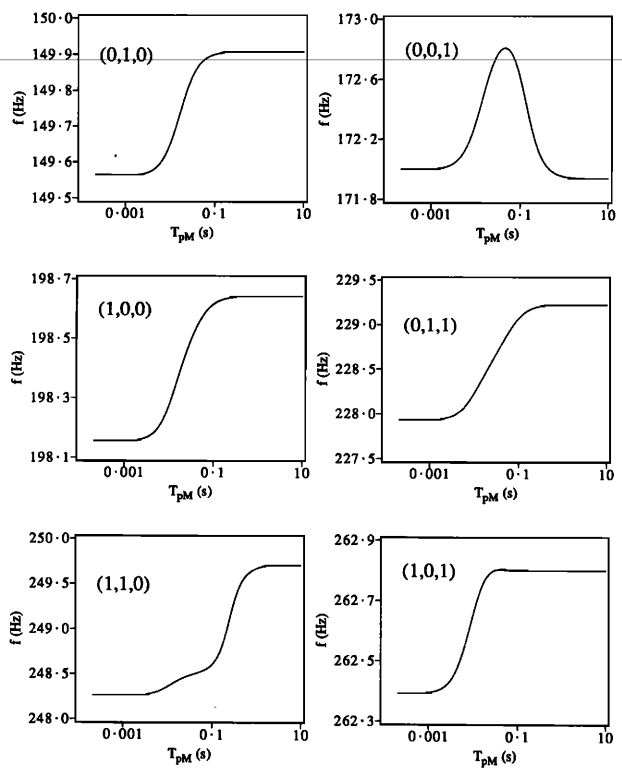

FIG. 10. Resonance frequencies of cavity-controlled modes as a function of panel modal decay time ($h = 6$ mm; $T_{aN} = 15.0$ s).

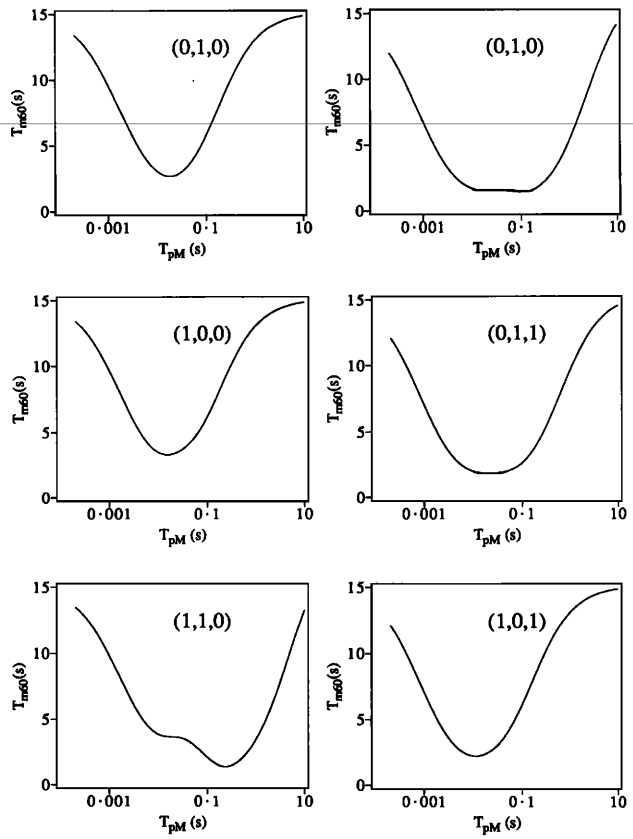

FIG. 11. Decay times of the cavity-controlled modes as a function of panel modal decay time ($h = 6$ mm; $T_{aN} = 15.0$ s).

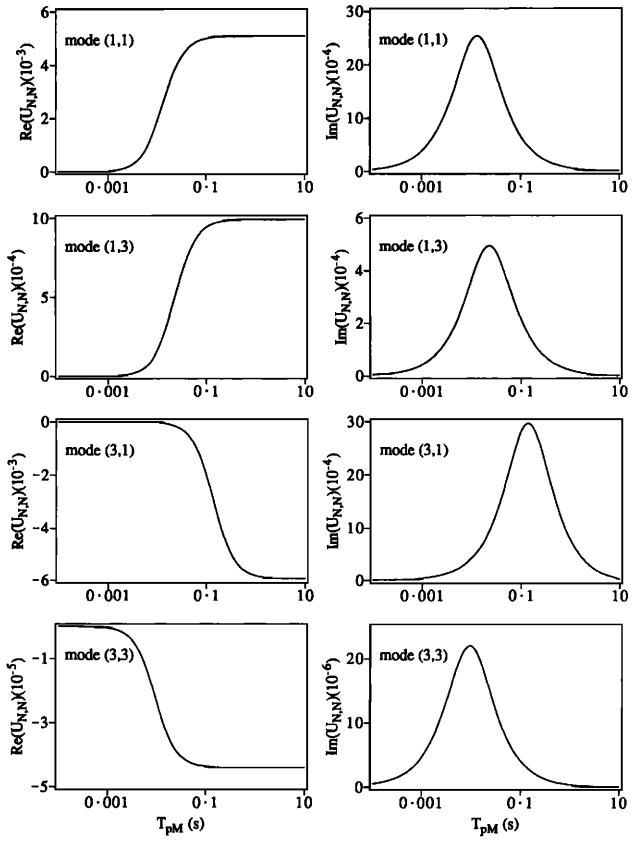

FIG. 12. Real and imaginary parts [$\mathrm{Re}(U_{N,N})$, $\mathrm{Im}(U_{N,N})$] of the components in $U_{N,N}$ as a function of panel modal decay time T_{pM} [$N = (0,0,1)$].

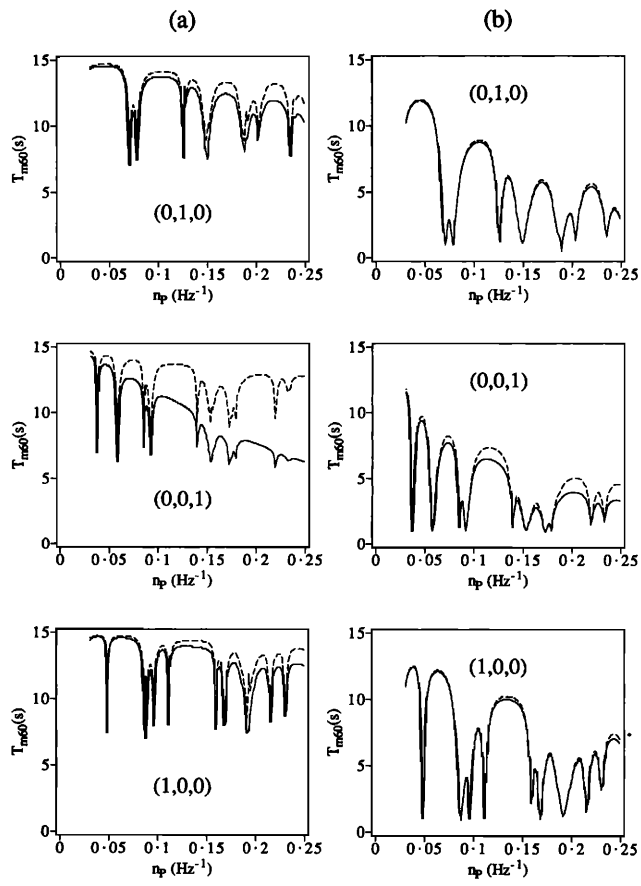

FIG. 13. Effect of panel radiation on the decay times of cavity-controlled modes; —, with radiation effect; - - -, without radiation effect ($T_{aN} = 15.0$ s). (a) $T_{pM} = 5.0$ s, (b) $T_{pM} = 0.5$ s.

(3,1) panel modes has comparable amplitudes but opposite signs. The net effect is to *slightly* reduce the resonance frequency. As panel damping increases ($T_{pM} \approx 0.1$ s), the influence of the (3,1) panel mode disappears, and only the effect of the (1,1) mode, which increases the resonance frequency, remains. As the panel damping increases further ($T_{pM} \approx 0.01$ s), the panel behaves as a rigid wall. Neither panel mode will affect the resonance frequency and the (0,0,1) acoustical mode degenerates into the (0,0,1) cavity mode. Figure 12 also shows the imaginary part of the first few terms of $U_{N,N}$ for (0,0,1) cavity-controlled mode. The large peak values for the (1,1) and (3,1) modes are responsible for the two minima in the resulting modal decay time curve of the (0,0,1) mode (Fig. 11).

D. Panel radiation

In previous studies of the structural–cavity coupling problem, external radiation from the panel was assumed to be negligible.[4,7] Up to this point, the effect of panel radiation upon the characteristics of the acoustical modes has been neglected. In this section, this effect will be incorporated into the calculation of the eigenvalues (i.e., resonance frequencies and modal decay times). Comparison with the results that exclude panel radiation effect reveals the conditions determining the importance of external panel radiation.

The influence of panel radiation can be included in the calculation of the complex eigenvalues of the cavity-controlled modes by adding an extra term Δ_N^{Pr} [given by Eq. (35)] to Eq. (29). The virtual mass terms $\sigma_{\mathrm{Im}}(M,N)$ are neglected from Eq. (35) and the radiation efficiency $\sigma_{\mathrm{Re}}(M,N)$ for the Nth cavity-controlled mode is estimated at the resonance frequency of the Nth cavity mode.

The 60-dB decay times of the first three cavity-controlled modes are shown in Fig. 13 as a function of panel modal density. In (a), the decay times of the cavity modes and the panel modes are 15 and 5 s, respectively. The curves obtained by considering the panel radiation modification term are shown as solid lines. Comparison of the dashed curves (neglecting panel radiation) with the solid curves shows that the panel radiation contribution to the modal decay times increases as the panel modal density increases (or as the panel thickness decreases).

According to the mass law for sound transmission loss,[47] the sound transmission loss through a panel decreases as the panel thickness decreases. This means that more energy is transmitted through the panel to external space. This increased energy loss to the external space results in increased sound absorption by the panel, and so decreased modal decay times.

The effect of the panel radiation upon the modal decay time is different for different cavity-controlled modes. For example, the decay time of the (0,0,1) cavity-controlled

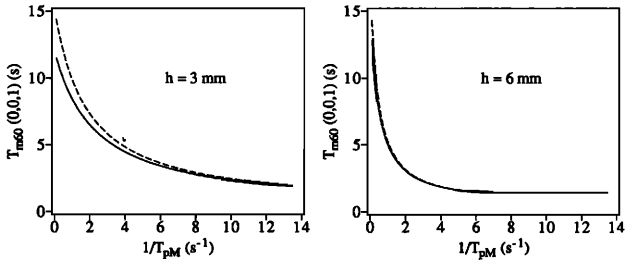

FIG. 14. The decay time of (0,0,1) cavity-controlled mode as a function of reciprocal panel modal decay time with (—) and without (- - -) radiation effect ($T_{aN} = 15.0$ s).

mode is more strongly affected by the panel radiation than other modes shown in Fig. 13(a). The panel vibration part of (0,0,1) cavity-controlled mode is dominated by volume displacement panel modes ("odd–odd" modes), such as (1,1) and (3,1). These volume displacement modes have higher radiation efficiencies.[48] Figure 13(b) shows the modal decay times of the same modes as in Fig. 13(a) except that the input decay times of the panel modes have been decreased to 0.5 s. In this case, the panel damping increases, and the contribution of the sound radiation of the panel is less important.

In the previous calculations, the panel decay times were fixed at 5.0 and 0.5 s in (a) and (b), respectively. Figure 14 shows the influence of panel radiation on the decay time of the (0,0,1) cavity-controlled mode as a function of reciprocal panel decay time. Both this result and that given in Fig. 13(b) show that the panel radiation has only minor effect on the decay times when the panel decay time is 0.5 s.

V. DISCUSSION AND CONCLUSIONS

The tradition description of a sound field in an enclosure isolates the sound field from the motion of the enclosing structure and from the external sound field; the influence of the bounary is modeled as a locally reactive acoustical impedance. By contrast, this article describes the sound field in a cavity in terms of the coupling in a panel–cavity system. Coupling with the external space is also considered as a perturbation effect.

In order to correctly describe the sound field in an enclosure with modally reactive boundaries, it is necessary to consider the internal sound field, the vibration of the boundaries and the external sound field as a single coupled system. In this system, the sound field in the enclosure cannot be modeled in isolation. The acoustical behavior of the whole system is described by acoustical modes, each of which has a sound field part and a boundary vibration part.

A modal coupling analysis has been used to investigate the free vibration of a coupled panel–cavity system. Numerical tests of this method show that the approximate solution converges rapidly and that the coupling of the panel with the cavity is weak. This approach allows calculation of the characteristics of the acoustical modes from the properties of the uncoupled cavity modes and panel mode (which are themselves based on fundamental parameters of the cavity and the panel). The geometry of the cavity and the boundaries used in this analysis is very simple, but the method of modal coupling does not, in fact, constrain the analysis to simple geometries. The low-frequency modal behavior of a complicated enclosure can be estimated in a similar way. Numerical methods are available for finding the mode shapes of any uncoupled enclosure and boundary structures.

Modal decay times characterize the transient behavior of a system. If a sound source drives a sound field at a resonance frequency of an acoustical mode (provided that the source is not located at a node of the mode), the sound field will decay at the decay rate of that mode. If the sound field is driven at an off-resonance frequency, or by a band of noise, the decay response will contain contributions from more than one mode. The decay behavior of an enclosure can be obtained by analysis similar to that of Hung *et al.*[49] Hunt's result depends only upon the cavity modes, but the results presented here are influenced by both the cavity modes and the panel vibrations. The participation of the sound field part of panel-controlled modes is not predicted by the classical model, but it can be important. The sound field component of a cavity-controlled mode can combine to form beating decays and double decay rates.

The model decay times of the system are related to the coupling coefficients, the distribution of resonance frequencies, the panel modal density, the panel damping, and the panel radiation loss to external space. The following five conclusions can be made.

(1) The matching or mismatching of the uncoupled mode shapes on the interacting surface of the sound field and boundary determines the possible energy transfer between two modes. The coupling coefficients, Eq. (18), are a measure of this matching.

(2) If the mode shapes of two uncoupled modes are well matched ($B_{M,N} \neq 0$), the difference between their resonance frequencies determines the rate of energy transfer. By adjusting (or tuning) this frequency difference, different modal decay times can be obtained. The smaller this difference is, the smaller is the modal decay time (provided that the decay rates of the uncoupled cavity modes are smaller than those of the uncoupled panel modes). The strength of interaction between two modes can be expressed as a transfer factor $F_{M,N}$. On average, the modal decay times of low-frequency, cavity-controlled modes decrease as panel modal density increases.

(3) The resonance frequency of a cavity-controlled mode can be different from that of its corresponding cavity mode. A panel mode with a particular resonance frequency will tend to "push away" (i.e., change the frequency of) the cavity modes with which it interacts.

(4) As the panel modal damping is increased, the decay time of each cavity-controlled acoustical mode first decreases to a minimum value, and then increases, eventually reaching the "rigid wall" value.

(5) If the panel is thin and its damping is low, radiation into the external space is an important cause of sound energy loss in the cavity. Otherwise, the effect of radiation upon modal decay times is negligible. Radiation by a boundary structure into external space can be large if an internal cavity mode is well coupled with a panel mode.

[1]P. M. Morse, "Some aspects of the theory of room acoustics," J. Acoust. Soc. Am. **11**, 56–66 (1939).
[2]J. Pan and D. A. Bies, "An experimental investigation into the interaction between a sound field and its boundaries," J. Acoust. Soc. Am. **83**, 1436–1444 (1988).
[3]E. H. Dowell and H. M. Voss, "The effect of a cavity on panel vibration," AIAA **1**, 476–477 (1963).
[4]A. J. Pretlove, "Free vibrations of a rectangular panel backed by a closed rectangular cavity," J. Sound Vib. **2**, 197–209 (1965).
[5]A. J. Pretlove, "Note on the virtual mass for a panel in an infinite baffle," J. Acoust. Soc. Am. **38**, 266–270 (1965).
[6]A. J. Pretlove, "Acousto-elastic effect in the response of large windows to sonic bangs," J. Sound Vib. **9**, 487–500 (1969).
[7]R. W. Guy, "The response of a cavity backed panel to external airborne excitation: A general analysis," J. Acoust. Soc. Am. **65**, 719–731 (1979).
[8]R. H. Lyon, "Noise reduction of rectangular enclosures with one flexible wall," J. Acoust. Soc. Am. **35**, 1791–1797 (1963).
[9]A. J. Pretlove, "Forced vibrations of a rectangular panel backed by a closed rectangular cavity," J. Sound Vib. **3**, 252–261 (1966).
[10]T. Khilman, "Sound radiation into a rectnagular room. Applications to airborne sound transmission in buildings," Acustica **18**, 11–20 (1967).
[11]M. C. Bhattacharya and M. J. Crocker, "Forced vibration of a panel and radiation of sound into a room," Acustica **22**, 275–294 (1969/70).
[12]M. C. Bhattacharya, "The transmission and radiation or acousto-vibration energy," Ph.D thesis, Department of Building Science, University of Liverpool (1970).
[13]E. H. Dowell, G. F. Gorman, and D. A. Smith, "Acoustoelasticity: general theory, acoustic nature modes and forced response to sinusoidal excitation, including comparisons with experiments," J. Sound Vib. **52**, 519–542 (1977).
[14]R. W. Guy and M. C. Bhattacharya, "The transmission of sound through a cavity backed finite plate," J. Sound Vib. **27**, 207–223 (1973).
[15]R. W. Guy, "The steady state transmission of sound at normal and oblique incidence through a thin panel backed by a rectangular room—a multi-modal analysis," Acustica **43**, 295–304 (1979).
[16]S. Naryannan and R. L. Shanbhag, "Sound transmission through elastically supported sandwich panels into a rectangular enclosure," J. Sound Vib. **77**(2), 251–270 (1981).
[17]S. Naryannan and R. L. Shanbhag, "Acoustoelasticity of a damped sandwich panel backed by a cavity," J. Sound Vib. **78**(4), 453–473 (1981).
[18]C. R. Fuller and F. J. Fahy, "Characteristics of wave propagation and energy distribution in cylindrical elastic shells filled with fluid," J. Sound Vib. **81**, 501–518 (1982).
[19]C. R. Fuller, "Analytical model for investigation of interior noise characteristics in aircraft with multiple propellers including synchrophasing," J. Sound Vib. **109**, 141–156 (1986).
[20]L. D. Pope, D. C. Rennison, C. M. Willis, and W. R. Mayes, "Development and validation of preliminary analytical models for aircraft interior noise prediction," J. Sound Vib. **82**, 541–575 (1982).
[21]L. D. Pope, E. G. Wilby, C. M Willis, and W. R. Mayes, "Aircraft interior noise models: sidewall trim stiffened structures and cabin acoustics with floor partition," J. Sound Vib. **89**, 371–417 (1983).
[22]M. C. Junger and D. Feit, *Sound, Structures and Their Interaction* (MIT, Cambridge, MA, 1986), 2nd ed.
[23]G. M. L. Gladwell and G. Zimmermann, "On energy and complementary energy formulation of acoustic and structural vibration problems," J. Sound Vib. **3**, 233–241 (1966).
[24]A. Craggs, "The transient response of a coupled plate-acoustic system using plate and acoustic finite elements," J. Sound Vib. **15**, 509–528 (1971).
[25]A. Craggs, "The use of simple three-dimensional acoustic finite elements for determining the natural modes and frequencies of complex shaped enclosures," J. Sound Vib. **23**, 331–339 (1972).
[26]A. Sestieri, D. D. Vescovo, and P. Lucibello, "Structural-acoustic couplings in complex shaped cavities," J. Sound Vib. **96**, 219–233 (1984).
[27]S. H. Sung and D. J. Nefske, "A coupled structural-acoustic finite element model for vehicle interior noise analysis," Tran. ASME. (J. Vib. Acoust. Stress. Rel. Design) **106**, 314–318 (1984).
[28]D. J. Nefske, J. A. Wolf, Jr., and L. J. Howell, "Structural-acoustic finite element analysis of the automobile passenger compartment," J. Sound Vib. **80**, 247–266 (1982).
[29]R. Rogers, "The absorption of sound by vibrating plates blocked with an air space," J. Acoust. Soc. Am. **10**, 280–287 (1939).
[30]J. W. Strutt Lord Rayleigh, *Theory of Sound* (MacMillan, London, 1896), 2nd ed., Vol. 2, p. 107.
[31]H. Feshbach, "On the perturbation of boundary conditions," Phys. Rev. **65**, 307–318 (1944).
[32]P. M. Morse and H. Feshbach, *Methods of Theoretical Physics* (McGraw-Hill, New York, 1953), pp. 1435–1440.
[33]P. M. Morse and R. H. Bolt, "Sound waves in rooms," Rev. Mod. Phys. **16**, 69–150 (1944).
[34]E. H. Dowell, "Reverberation time, absorption and impedance," J. Acoust. Soc. Am. **64**, 181–191 (1978).
[35]J. C. Snowdon, "Forced vibration of internally damped circular plates with supported and free boundaries," J. Acoust. Soc. Am. **47**, 882–891 (1970).
[36]G. L. Anderson, "Application of a variational method to dissipative, nonconservative problems of elatic stability," J. Sound Vib. **27**, 279–296 (1973).
[37]*IMSL Library*—FORTRAN subroutines for mathematics and statistics (IMSL, Houston, TX, 1985).
[38]J. Pan, "A new look at the description of reverberant spaces," Ph.D thesis, Department of Mechanical Engineering, Univerity of Adelaide, Australia 132–137 (1988).
[39]C. E. Wallace, "Radiation resistance of a rectangular panel," J. Acoust. Soc. Am. **51**, 946–952 (1972).
[40]F. G. Leppington, E. G. Broadbent, and K. H. Heron, "The acoustic radiation efficiency of rectangular panels," Proc. R. Soc. London Ser. A **382**, 245–271 (1982).
[41]L. D. Pope and J. F. Wilby, "Band-limited power flow into enclosures," J. Acoust. Soc. Am. **62**, 906–911 (1977).
[42]F. J. Fahy, A. Majid, and J. H. Howlett, "Acoustic coupling between structure and liquids," Annu. Rep. I.S.V.R., University of Southampton **76** (1970).
[43]R. H. Lyon and G. Maidanik, "Power flow between linearly coupled oscillators," J. Acoust. Soc. Am. **34**, 623–639 (1962).
[44]F. J. Fahy, "Vibration of containing structures by sound in the contained fluid," J. Sound Vib. **10**, 490–512 (1969).
[45]W. H. Louisell, "Coupled mode and parametric electronics" (Wiley, New York, 1960).
[46]P. M. Morse and K. U. Ingard, *Theoretical Acoustics* (McGraw-Hill, New York, 1968), Chap. 6, pp. 259–270.
[47]I. L. Vér and I. H. Curtis, *Noise and Vibration Control*, edited by L. L. Beranek (McGraw-Hill, New York, 1971), Chap. 11.
[48]F. J. Fahy, *Sound and Structural Vibration: Radiation, Transmission and Response* (Academic, New York, 1985), Chap. 2, pp. 66–67.
[49]F. V. Hunt, L. L. Beranek, and D. Y. Maa, "Analysis of sound decay in rectangular rooms," J. Acoust. Soc. Am. **11**, 80–94 (1939).